MJFAS
Malaysian Journal of Fundamental and Applied Sciences

Othman *et al.* | Malaysian Journal of Fundamental and Applied Sciences, Vol. 22 (2026) 199–214

RESEARCH ARTICLE

Predictive Modeling of Globule Size Distribution in Double Emulsions Stabilized by Blended Surfactants and Nanoparticles using Hinze-Kolmogorov Theory

Norasikin Othman[a,b]*, Tan Yi Hao[a], Norul Fatiha Mohamed Noah[a], Norela Jusoh[a], Izzat Naim Shamsul Kahar[a], Sazmin Sufi Suliman[a], Shuhada A. Idrus-Saidi[a,b], Aishah Rosli[a,b]

[a]Faculty of Chemical and Energy Engineering, Universiti Teknologi Malaysia, UTM, 81310 Skudai, Johor Bahru, Malaysia; [b]Centre of Lipids Engineering and Applied Research (CLEAR), Ibnu Sina Institute for Scientific and Industrial Research, Universiti Teknologi Malaysia, 81310 UTM Johor Bahru, Johor, Malaysia

Abstract Emulsion liquid membrane (ELM) is a promising approach for heavy metal extraction. Its effectiveness depends strongly on emulsion stability, which is largely controlled by the globule size of the water-in-oil-in-water (W/O/W) or double emulsion. In this study, the Hinze-Kolmogorov theory was assessed as a predictive modeling for estimating the Sauter mean diameter (D_{32}) of W/O/W globules formulated with blended surfactants and nanoparticles, and its applicability was demonstrated using zinc extraction data. Two linear regression relationships were established in MATLAB utilizing nonlinear programming solver 'fminsearch' function, one based on agitation speed (Case 1) and the other on holdup fraction (Case 2) and were used to determine the Hinze Kolmogorov constants C_1 and C_2. The resulting empirical correlation, with C_1 = 0.0436 and C_2 = −3.2561, showed strong agreement with experiments with average absolute relative deviation (AARD) ≤ 5% and coefficient of determination (R^2) ≥ 0.85, enabling direct estimation of D_{32} across the tested operating conditions. Using this validated correlation, the effects of impeller diameter, agitation speed, interfacial tension, and holdup fraction were systematically evaluated. The analysis indicates that increasing impeller diameter and agitation speed reduces globule size, while lower interfacial tension and higher holdup fractions further promote the formation of smaller globules. Overall, the proposed correlation provides a practical tool to guide ELM process by enabling globule size control for zinc extraction applications.

Keywords: Emulsion liquid membrane, Hinze-Kolmogorov theory, emulsion stability, globule size prediction, W/O/W emulsion.

***For correspondence:**
norasikin@cheme.utm.my

Received: 14 Nov. 2025
Accepted: 10 Jan. 2026

Introduction

The rapid industrialisation of the 21st century has led to an increase in heavy metals wastewater, causing a substantial impact on the pollution of natural water reservoirs. Zinc is one of the heavy metals that significantly contribute to water pollution. Typically, less than 1 ppm or up to more than 48,000 ppm of zinc can be found in wastewater [1]. According to the Environmental Quality (Industrial Effluent) Regulations 2009 issued by the Department of Environment Malaysia, the permissible limit for zinc in industrial effluents is 2 mg/L [2]. Therefore, the removal of zinc from wastewater is crucial to prevent its toxic effects on human health and hazardous impact on aquatic systems.

There are various methods that have been reported for zinc removal, including solvent extraction, ion exchange, adsorption, and chemical precipitation. Solvent extraction is an effective method for zinc removal, offering high selectivity and the ability to recover zinc from complex matrices. Despite these

advantages, its application is limited by solvent loss, high operational costs, and environmental concerns [3]. Another method used for heavy metal removal is ion exchange. This method can remove zinc ions and completely deionise a solution or substance. Unfortunately, this method may cause fouling and regeneration, as well as bacterial contamination [4]. Meanwhile, adsorption is a promising method for zinc removal, offering simplicity, low cost, and the use of various natural or synthetic adsorbents. Nevertheless, its performance can be limited by low adsorption capacity, slow kinetics, and the need for regeneration or disposal of spent adsorbents [5]. Chemical precipitation is a widely employed technique for the elimination of heavy metals. However, there are several drawbacks to this approach, including its high chemical consumption, considerable sludge production, and incapability to extract heavy metals at low concentrations [6]. Thus, several researchers have turned their interest to a novel and sustainable method, which is liquid membrane technology.

Emulsion liquid membrane (ELM) process is one of the liquid membrane technologies that has piqued interest among researchers due to its simplicity, rapid extraction, simultaneous extraction and stripping, versatility, as well as the small amount of chemical and energy required [7, 8]. The ELM process is a three-phase system consisting of water-in-oil-in-water (W/O/W) emulsion, also known as double emulsion system. In this system, the layer that separates the two water phases is referred to as the liquid membrane phase.

While this technology has numerous benefits, the stability of the ELM process needs to be considered since it may reduce the effectiveness of the zinc removal [9]. Breakage, coalescence, flocculation, and creaming are the phenomena that could cause the instability of the W/O/W emulsion. The instability can be minimised by varying surfactant concentration. Nonetheless, excessive surfactant concentration is not recommended since it would cause swelling and breakage due to the increased water transportation into the emulsion globules [10]. Alternatively, the W/O/W emulsion embedded with blended surfactant-nanoparticle can prevent the emulsions from coalescing and enhance the emulsion stability [7, 11]. This is because nanoparticles can adsorb at the oil-water (O/W) interface and stabilise the emulsions for extended periods [12, 13]. Recently, several studies have focused on particle-stabilised emulsions using different nanoparticles including iron (III) oxide (Fe_2O_3) [9], silica [14], hydroxyapatite [15], and cetyl trimethyl ammonium bromide (CTAB) cationic surfactant [16].

Due to the increased interest in the ELM process, several researchers have suggested simulating the mass transfer of ELM as well as predicting emulsion size [17, 18]. It is important to tune the stability of the ELM to improve the efficiency of extraction. Studies have demonstrated that emulsions' sizes are closely associated with ELM stability and can be estimated using correlation models [19, 20]. The Hinze-Kolmogorov theory is typically employed to derive the correlation for Sauter mean diameter (D_{32}) in a mixer vessel, as it evaluates the size of droplets in turbulent fluids and considers the droplet disintegration process. Large-scale eddies are the energy input into the system during fully developed turbulence, and these eddies cascade towards a smaller scale, producing the energy spectrum's Kolmogorov power law. Large-size droplets in these turbulent fluids are unstable because the fluctuating pressure of the surrounding fluid can cause them to deform and disintegrate. Large droplets thus break into smaller droplets, and this process of breaking continues until a balance is reached where the turbulent energy needed to break the droplets up equals the droplet energy needed to maintain their shape [21]. The general structure of the Hinze-Kolmogorov theory is shown in Equation 1:

$$\frac{D_{32}}{D_I} = C_1(1 + C_2\phi)We^{-0.6} \quad (1)$$

where C_1 and C_2 are constants, and ϕ is the holdup or dispersed phase volume fraction. The Weber number (We) is dimensionless, which is affected by the emulsification apparatus and is frequently employed for scaling up at geometric similarity, as defined by Equation 2:

$$We = \frac{\rho_C N^2 {D_I}^3}{\sigma} \quad (2)$$

where ρ_C is the density of the continuous feed phase, N is the agitation speed, D_I is the impeller diameter, and σ is the interfacial tension. Apart from that, the volume displacement method was used to determine the holdup fraction of primary water-in-oil (W/O) emulsion, ($\emptyset i$), as shown in Equation 3:

$$\emptyset i = \frac{V_d}{V_d + V_o} \quad (3)$$

where V_d denotes the volume of the dispersed phase and V_o refers to the volume of the organic phase.

Table 1 shows the relevant predictive correlations for D_{32} developed for different chemical systems and surfactants and a few parameters that follow the general equation from Hinze-Kolmogorov theory. Hinze-Kolmogorov models for predicting globule size in ELM are based on assumptions of homogeneous turbulence and uniform energy dissipation and do not account for dynamic phenomena such as globule breakage, coalescence, or time-dependent emulsion stability. Furthermore, these models are typically constrained to optimal dispersed phase holdup and specific surfactant-nanoparticle formulations, limiting their predictive capability under varying operating conditions or during scale-up. Incorporating mechanisms of globule breakage and coalescence into the model is expected to enhance prediction accuracy and provide a more realistic representation of emulsion stability, thereby supporting improved design and optimization of ELM process.

Previous work investigated zinc removal using ELM with blended surfactant and nanoparticles. However, a predictive model linking operating conditions to W/O/W emulsion globule size (D_{32}), which is a key indicator of ELM stability, has not been reported for this system. Here, we predict and validate globule size using Hinze–Kolmogorov theory and then use the model to identify how mixing and formulation choices (e.g., impeller size, agitation speed, interfacial tension, holdup fraction) control globule size and stability. Model validation was performed using experimental data reported by Suliman et al. [7].

Table 1. Summary of several correlations in liquid-liquid dispersions based on Hinze-Kolmogorov theory

Chemical System	Type of impeller	Correlations	Refs.
Toluene in ether dispersion Surfactant: Aniline	Spiral impeller	$\frac{D_{32}}{D_I} = 0.453(1 + 0.612\,\phi) \times \left[1 + 2215.137\,V_I\left(\frac{D_{32}}{D_I}\right)^{0.828}\right] We^{-0.603}$ $\frac{D_{32}}{D_I} = 0.467(1 + 0.224\,\phi) \times \left[1 + 27176.9\,V_I\left(\frac{D_{32}}{D_I}\right)^{1.926}\right] We^{-0.509}$	[22]
Five liquid-liquid systems using different surfactants	6-blade flat-blade turbine impeller	$\frac{D_{32}}{D_I} = 0.05\,C_s(1 + 2.316\,\phi) \times We^{-0.6} Fr^{-0.13}\left(\frac{D_I}{D_T}\right)^{-0.75}$	[23]
Silicone oil in water dispersion Surfactant: SLES	6-blade flat-blade turbine impeller	$\frac{D_{32}}{D_I} = 0.053\left(1 + 4.42\,V_I^{0.79}\right)^{0.6} We^{-0.6}$	[24]
$NiCl_2$ in (combination of Solvesso 150 and TBP)	4 blades pitched	$\frac{D_{32}}{D_I} = 0.28(1 + 0.29\,\phi) We^{-0.6}$	[25]
HCl in (combination of Solvesso 150 and TBP)	4 blades pitched	$\frac{D_{32}}{D_I} = 0.14(1 + 0.48\,\phi) We^{-0.6}$	[25]
Mean drop size (D_{32}) in a horizontal mixer-settler for a toluene/water system	10 mm dispersing tool (manufactured by IKA)	$\frac{D_{32}}{D_I} = 0.055(1 + 0.862\,\phi)(1 + \omega)^{-1.994} We^{-0.6}$	[15]
Toluene in water dispersion Surfactant: SDS	Spiral impeller	$\frac{D_{32}}{D_I} = 0.56(1 + 1.55\,\phi) We^{-0.52}$	[26]
W/O/W (acid thiourea/palm oil/zinc solution) Blended surfactant-nanoparticles (Span 80-Fe_2CO_3)	4 blades pitched	$\frac{D_{32}}{D_I} = 0.0436\,[1 + (-3.2561\,\phi)]\,We^{-0.6}$	This work

Materials and Methods

Data Collection for Model Validation

The parameters required to develop the predictive model for emulsion globules size involved four parameters: organic-to-internal (O/I) ratio, agitation speed, agitation time, and treat ratio, as shown in

Table 2. The range of parameters were selected based on previous studies. Meanwhile, Table 3 presents the optimum primary emulsion operating conditions used in ELM zinc removal [18].

Table 2. Parameters used in the proposed modelling [7, 18, 27]

No.	Parameters	Range
1	(O/I) Ratio	1:1, 1.25:1, 1.35:1, 1.75:1
2	Agitation Speed (s^{-1})	3.33, 5.00, 6.67, 8.33
3	Agitation Time (min)	1, 3, 5, 7, 10
4	Holdup Fraction	0.091 – 0.25

Table 3. Operating conditions for predictive globule size model

Conditions	Value
Homogenizer speed	133.33 s^{-1}
Emulsifying time	3 min
Modifier (octanol)	3% (w/v)
Acidic thiourea (0.1:0.45)	1.375 M
D2EHPA/Cyanex 302 (9:1)	0.03 M
Mixed surfactant (Span 80 and Tween 80)	HLB 8, 5% (w/v)
Nanoparticle (Fe_2O_3)	0.02% (w/v)
Interfacial tension W/O and external feed phase	2 mN/M
Surface tension for external feed phase (zinc)	70 mN/m

Equation 3 is applicable exclusively to primary emulsions and is utilised for internal droplet fractions. For double W/O/W emulsion, external feed phase was involved, and the holdup fraction of double emulsion, $\emptyset ii$ was calculated using Equation 4:

$$\emptyset ii = \frac{V_d + V_o}{V_d + V_o + V_f} \quad (4)$$

where V_f represents the volume of the external feed phase.

ELM Model Assumptions

The emulsion instability involving breakage and swelling was taken into consideration in order to create an accurate mathematical model of ELM that would be valid over a wide range of parameters. The model was developed based on the following assumptions:

i. The size distributions of droplets (W/O) and globules (W/O/W) are indicated by the Sauter mean diameter.
ii. Since there is a sufficient number of surfactants, there is no internal circulation within the W/O/W emulsion, and the W/O are immobilised.
iii. There is no coalescence or redistribution in emulsion W/O/W.
iv. At both the internal and external feed-membrane interfaces, the distribution coefficient is the same.
v. The external feed phase is completely blended.
vi. The internal mass transfer resistance is negligible because the droplets are very small.
vii. Since the procedure is isothermal at perfect mixing, the physical properties remain constant during the recovery.
viii. Throughout the process, the density and pH value of the external feed phase remain constant.
ix. The quantity of W/O/W emulsion does not change even after emulsion breakage and swelling are considered. These hypotheses are derived from the emulsion breakup that takes place at the outermost droplets of the globules.

W/O/W Emulsion Globule Size Prediction using MATLAB Software

This study employs two cases in developing the predictive model in MATLAB software, as shown in Table 4 with different manipulated variables. Case 1 was executed by manipulating the agitation speed while fixing the O/I ratio, holdup fraction, agitation time, and temperature. Meanwhile, the manipulated

variable for Case 2 was the holdup fraction while the other parameters were held constant. Figs. 1 and 2 present the linear trendlines, demonstrating the relationship between the experimental D_{32} obtained from previous studies and the agitation speed and holdup fraction, respectively [7].

Table 4. Manipulated and constant variables used in different cases in MATLAB coding [7]

Case	Variables	Parameters	Range
1	Manipulated	Agitation speed (s^{-1})	3.33 – 5.00
	Constant	O/I Ratio	1.35:1
		Holdup Fraction	0.25
		Temperature (℃)	26 ± 1
		Agitation Time (min)	3
2	Manipulated	Holdup Fraction	0.25 – 0.091
	Constant	O/I Ratio	1.35:1
		Agitation Speed (s^{-1})	5.00
		Temperature (℃)	26 ± 1
		Agitation Time (min)	3

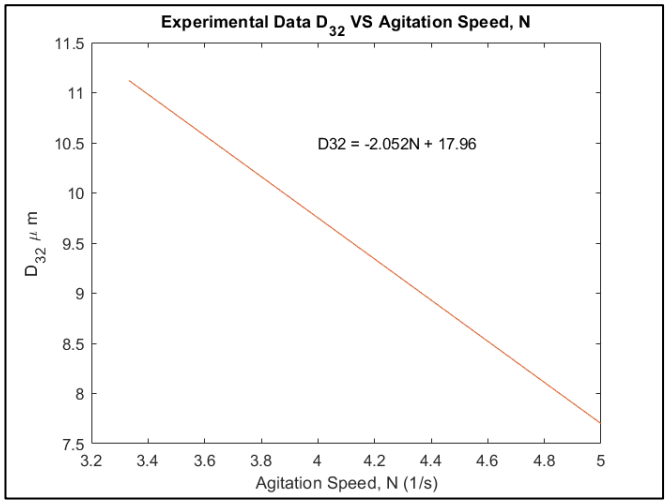

Figure 1. Relationship between experimental D32 with agitation speed

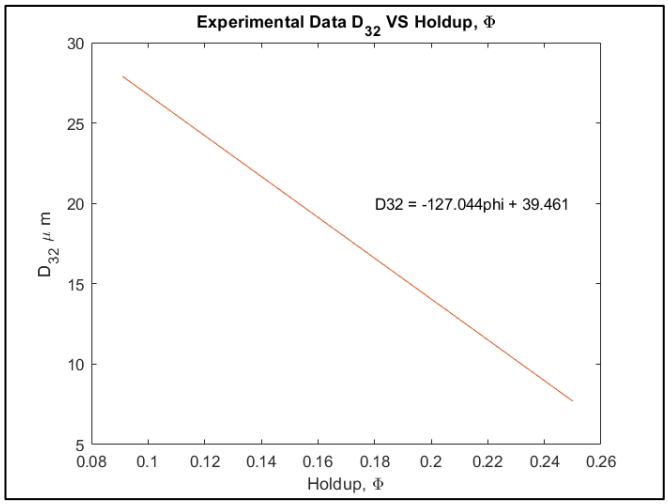

Figure 2. Relationship between experimental D32 with holdup fraction

The algorithmic steps of the MATLAB simulation for developing predictive model are shown in Fig. 3. The parameter values were initially defined and added to the programme script. Linear trendline equations from two parameters were inserted into the MATLAB *m-files* based on the generated mathematical models, and the known parameters were substituted into the linear trendline equation. The linear trendline equations were calculated simultaneously using the '*fminsearch*' solver in MATLAB and the globule size was simulated. '*fminsearch*' solver is a built-in optimisation algorithm in MATLAB that is widely used for finding the minimum of unconstrained multivariable functions [28]. The '*fminsearch*' function returns the ideal values of the parameters after receiving as inputs the goal function, the initial guess of the parameters, and additional parameters. Similarly, in this study, the primary objective is to find an optimal value that is suitable to plug into Equation 1 to provide a lower average absolute relative deviation (AARD) when predicting the globule emulsion size. Equation 5 was used to estimate the (AARD):

$$AARD = \frac{1}{NE}\sum_{i=1}^{NE}\left|\frac{(\mathrm{D}_{32})_{i,exp} - (\mathrm{D}_{32})_{i,calc}}{(\mathrm{D}_{32})_{i,exp}}\right| \quad (5)$$

where $(\mathrm{D}_{32})_{i,exp}$ is the Sauter mean diameter from the experimental data, and $(\mathrm{D}_{32})_{i,calc}$ is the calculated or predicted Sauter mean diameter based on the theory. The model is validated when AARD is less than 5%. Otherwise, the model is not validated, and the known parameters must be recalculated and redefined.

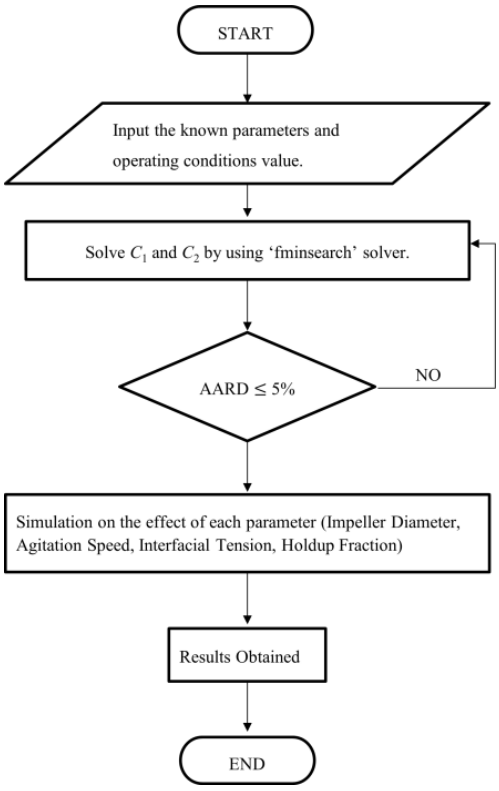

Figure 3. Algorithmic steps of the MATLAB simulation for developing predictive model

Results and Discussion

Validation of the Globule Size Prediction Model

The constant coefficients in Hinze-Kolmogorov theory were evaluated by the nonlinear programming solver '*fminsearch*' function in MATLAB R2024a software, as shown in Figs. 4 (a) and (b). The results in Fig. 4(a) show good agreement with the experimental data. In order to align with the Hinze-Kolmogorov theory and achieve consistency with most reported correlations for D_{32}, such as the silicone oil in water dispersion system [24] and the toluene/water system [14] (Table 1), the exponent of the Weber number

in Equation 6 was adjusted to −0.6. This adjustment was suggested as the estimated exponent (−0.4597) is relatively close to the theoretical value.

$$\frac{D_{32}}{D_I} = 0.0190\,[1 + (-3.2032\,\phi)]\,We^{-0.4597} \quad (6)$$

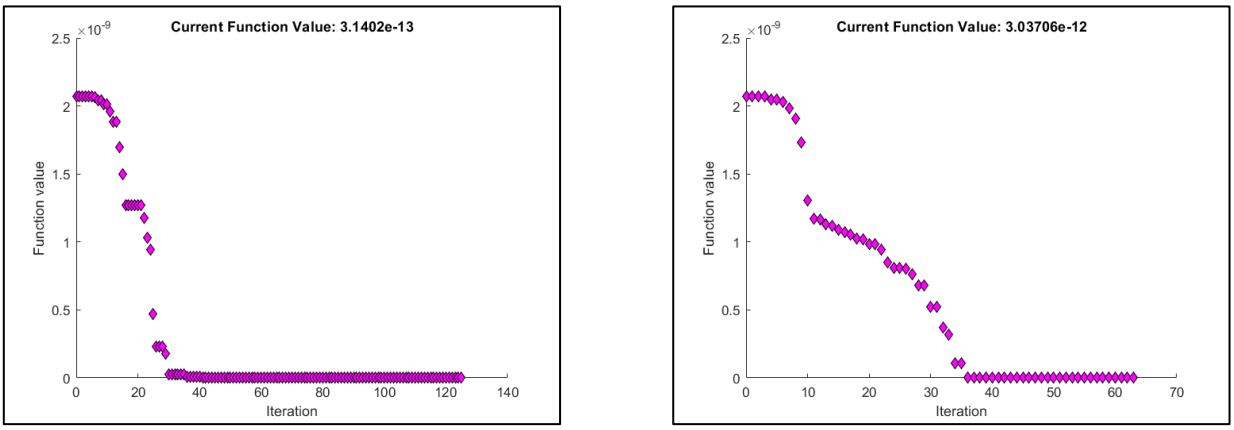

(a) (b)

Figure 4. Nonlinear programming solver, fminsearch function in MATLAB R2024a (a) before modification of exponent of Weber number (b) after modification of exponent of Weber number

After modifying the exponent of the Weber number, the constants (C_1 and C_2) were slightly adjusted, and the resulting correlation (Equation 7) yielded R^2 values of 0.8466 and 0.9994 for agitation speed and holdup fraction, respectively. The equation was validated based on the limitations and range of agitation speed and holdup fraction, as mentioned in Section 2.

$$\frac{D_{32}}{D_I} = 0.0436\,[1 + (-3.2561\,\phi)]\,We^{-0.6} \quad (7)$$

The predicted and actual D_{32} before and after modification of the exponent of the Weber number are shown in Figs. 5 and 6, respectively. The predicted D_{32} after the modification is quite similar to the experimental results. The illustration of the W/O/W emulsion formation in the experimental study is shown in Fig. 7. However, in Table 5, the %AARD after modification of the exponent of the Weber number increased slightly as compared to before, from 1.07% to 3.41%. Since the %AARD is still less than 5%, the results are considered acceptable and reliable. The derivative values are summarized in Table 5.

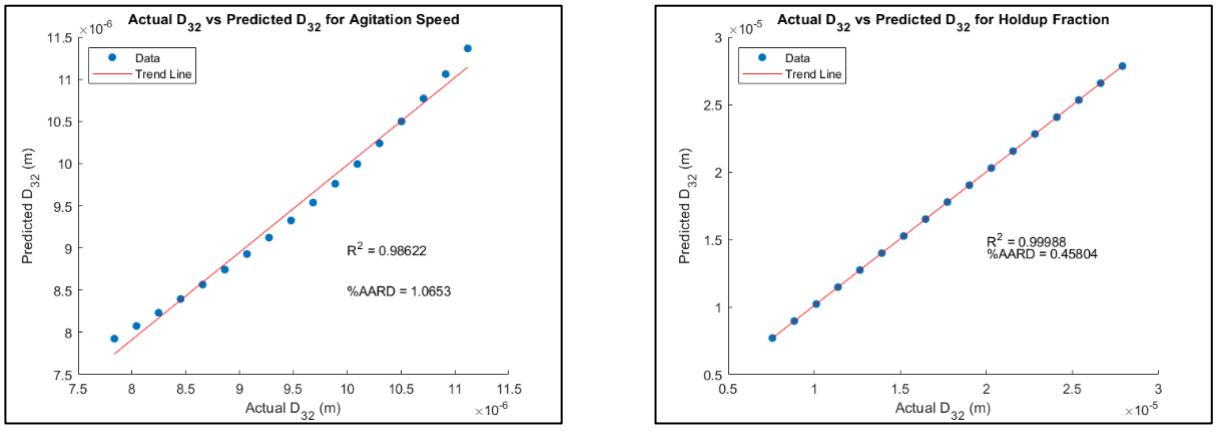

(a) (b)

Figure 5. Predicted D32 versus actual D32 before modification of exponent of Weber number for varied (a) agitation speed (b) holdup fraction

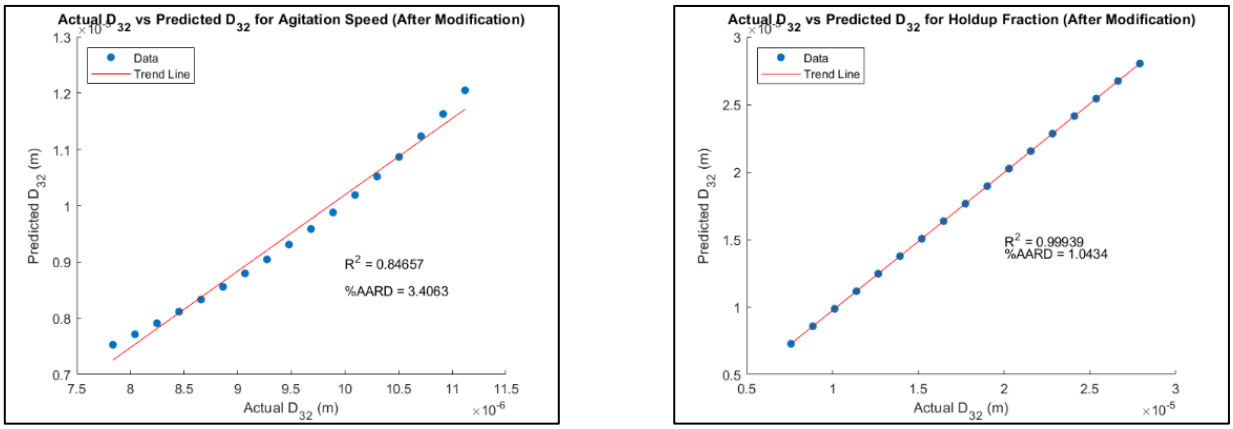

(a) (b)

Figure 6. Predicted D_{32} versus actual D_{32} after modification of exponent of Weber number (a) agitation speed (b) holdup fraction

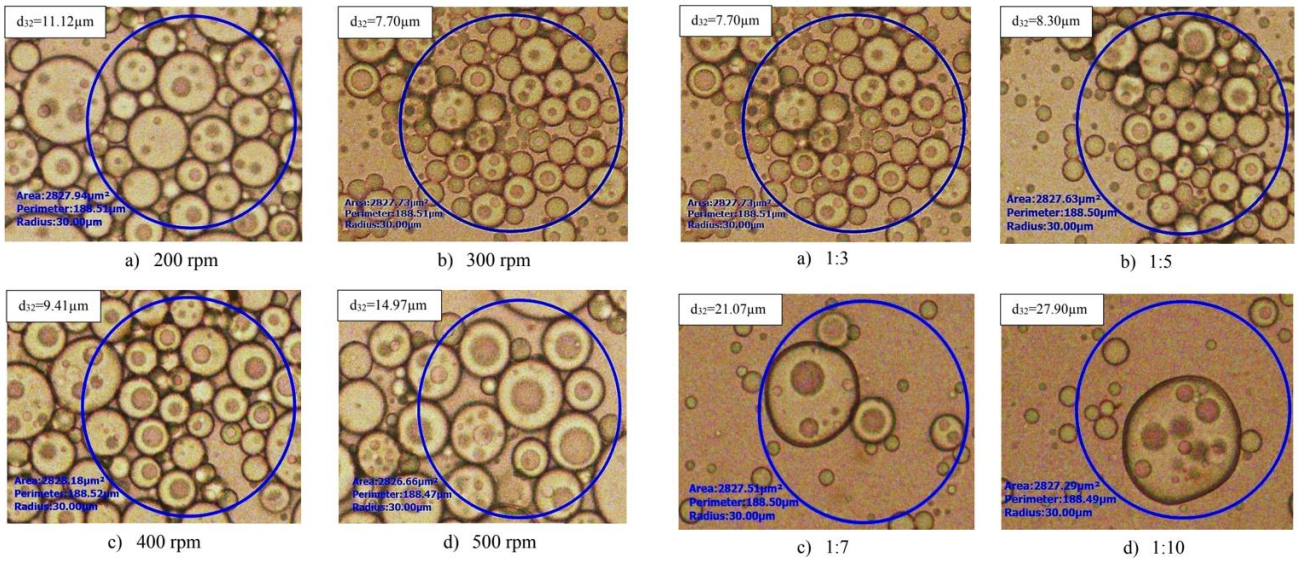

a) 200 rpm b) 300 rpm a) 1:3 b) 1:5

c) 400 rpm d) 500 rpm c) 1:7 d) 1:10

(i) (ii)

Figure 7. The illustration of the W/O/W emulsion formation in the experimental study (i) Effect of agitation speed; (ii) Effect of holdup fraction

Table 5. Calculation results for the functional form of Equations 6 and 7

Coefficient	Equation 6	Equation 7
C_1	0.0190	0.0436
C_2	-3.2032	-3.2561
n	-0.4597	-0.6
R^2 (Case 1: N)	0.9862	0.8466
%AARD (Case 1: N)	1.07	3.41
R^2 (Case 2: ϕ)	0.9999	0.9994
%AARD (Case 2: ϕ)	0.46	1.04

Parametric Study of ELM Process

Effect of Impeller Diameter

The effect of impeller diameter on the emulsion size in the ELM process was investigated in the range of 0.01–0.1 m as shown in Fig. 8. An increase in impeller diameter was found to reduce globule size due to the corresponding rise in shear rate, turbulence, and Weber number. This results in smaller, more homogeneous globules, thereby enhancing mass transfer and emulsion stability. The results obtained

are consistent with the outcomes of Ohtake et al. [29]. Typically, the higher the number of smaller emulsion globules and droplets, the greater the surface area for mass transfer [30]. As shown in the figure, globule size decreased with increasing impeller diameter up to a critical point, after which it reached a plateau with no further change. This suggests that when the fluid flow rate goes beyond a critical limit, turbulence happens once the impeller has supplied enough energy, resulting in the development of tiny eddies caused by the turbulence. As most of the energy is dissipated through viscous losses rather than emulsion disruption, the small eddies become ineffective, and further increasing the impeller diameter does not significantly influence the emulsion size [18].

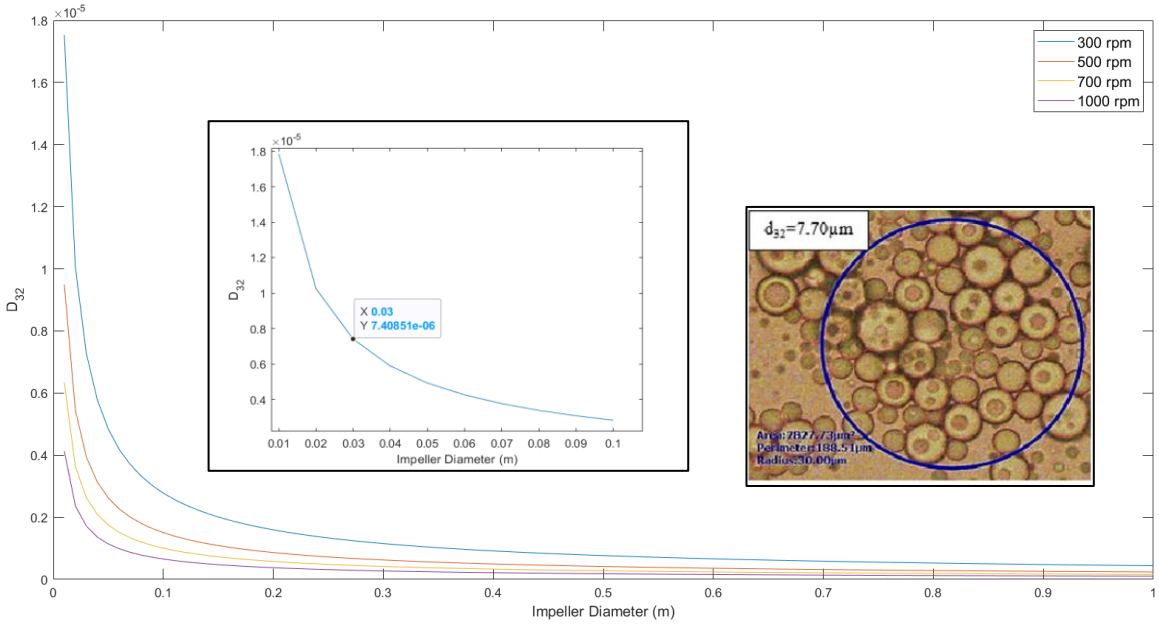

Figure 8. Effect of impeller diameter on globule size, D32. (Fixed conditions: interfacial tension: 2 mN/m; holdup fraction: 0.25; temperature: 26±1)

Additionally, the effect of impeller diameter at different agitation speeds (5.00 – 16.67 s^{-1}) on globule size was also examined. Based on the experimental result (inset image in Fig. 8), the agitation speed of 5.00 s^{-1} with an impeller diameter of 0.03 m resulted in an experimental globule size of 7.70 µm. Meanwhile, the predicted globule size from Equation 7 is 7.41 µm. The percentage error is only 3.77%, proving that the predicted emulsion globule size is close to the experimental results. On the other hand, when the impeller diameter is increased to 0.04 m, the size becomes 5.89 µm. The difference between globule sizes for impeller diameters of 0.03 m and 0.04 m is about 20.5%. Conversely, when the impeller diameter approaches 0.99 m and 1.0 m, the globule emulsion sizes are 0.4518 µm and 0.4482 µm, respectively. The difference for the globule emulsion sizes between these two diameters is less than 1%, meaning that the globules have achieved a stable state. At high agitation speeds (16.67 s^{-1}), the globule size is smaller compared to 11.67 s^{-1}. For instance, when the impeller diameter is 0.1 m, the globule sizes at 5.00 s^{-1} and 16.67 s^{-1} are 2.83 µm and 0.667 µm, respectively. The details regarding the effect of high agitation speeds on globule size are discussed in the following section.

Effect of Agitation Speed

The impact of agitation speed on globule size (D_{32}) in the ELM process was investigated in the range of 1.67 – 50 s^{-1} as shown in Fig. 9. It was found that a rise in agitation speed, which intensifies droplet breakage and increases the Weber number, resulted in smaller globules. Based on the developed correlation, the globule size is inversely proportional to agitation speed, which is consistent with experimental data. The observed relationship between agitation speed and globule size suggests that as agitation speed rises, more turbulence energy is created, expanding the breakup of globules and droplets and producing finer globules. These results are aligned with those by other researchers [14]. The smaller globules enhance the efficiency of extraction and stability of the ELM process [31]. The simulation results showed an 8.36% error at 3.33 s^{-1} as compared to experimental data. The simulation shows that when the impeller diameter is 0.03 m, the globule sizes at agitation speeds of 5 s^{-1} and 10 s^{-1} were 7.41 µm and 3.22 µm, respectively. The percentage difference between these two speeds is quite high, at 56.55%. On the other hand, at agitation speeds of 25.00 s^{-1} and 30 s^{-1}, the difference in

globule emulsion size is 19.65%, which is significantly smaller. Further increasing the agitation speed would make the emulsion stable in size. When the speed approaches 45 s^{-1} and 50 s^{-1}, the difference of D_{32} between the speeds is only 11.9%.

The study also found that each ELM system has an optimal range for impeller diameter and agitation speed. While the simulations show the results based on theory; it was noticed that in practice, globules and droplets tend to coalesce at certain speeds [7]. Beyond the critical point, the globule size increases due to excessive breakage and coalescence. These outcomes specify valuable insights for the design and optimisation of ELM processes.

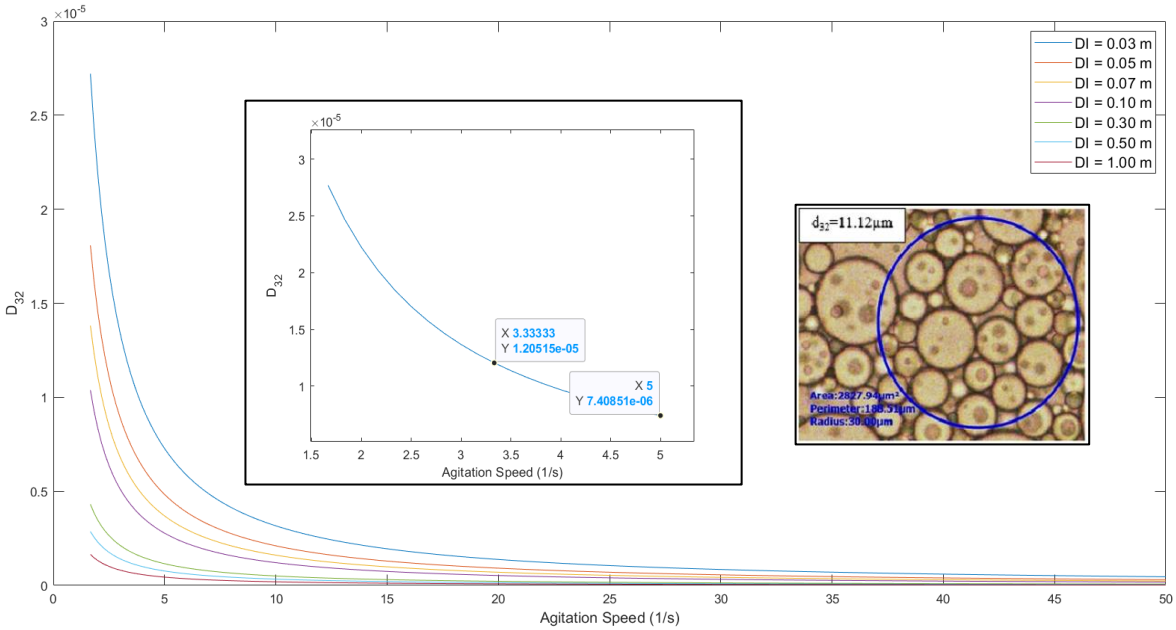

Figure 9. Effect of agitation speed on globule size, D32. (Fixed conditions: interfacial tension: 2 mN/m; holdup fraction: 0.25; temperature: 26±1°C)

Effect of Interfacial Tension on Different Types of Diluents

The effect of interfacial tension on globule size in the ELM process using different types of diluents was investigated. The diluents, such as palm oil with iron (III) oxide nanoparticles, toluene with silica nanoparticles, toluene with CTAB cationic surfactant, crude palm oil (CPO), dibutyl carbitol, and n-heptane, were compared in terms of the resulting globule size. The interfacial tensions for each diluent are presented in Table 6. It was found that low interfacial tension leads to smaller globules, as shown in Fig. 10. Palm oil with iron (III) oxide nanoparticles used by Suliman et al. [7] showed the smallest predicted globule size, which is 7.41 µm, with a value close to experimental results (7.70 µm). The presence of nanoparticles alters the interfacial tension during globule breakup by modifying the interfacial rheology and provide synergy to the surfactant [32]. Nanoparticles preferentially adsorb at the interfacial area, where a densely packed particle (bridge) was generated and reduces effective interfacial tension. This reduces the energy needed to generate droplets. The “bridging” mechanism also helps in maintaining the globules at a small distance, hence preventing the globules coalescence [33].

Different diluents have different interfacial tensions with water due to their varying chemical compositions and physical characteristics. According to Raji-Asadabadi et al. [14], the interfacial tension of toluene in the existence of silica nanoparticles is 32 mN/m. The results show that interfacial tension at this level produces large globules, which is 39.1 µm when the conditions like impeller diameter and agitation speed are kept constant as in the research of Suliman et al. [7]. However, when toluene is mixed with CTAB cationic surfactant, the interfacial tension with water is lower than when mixed with silica nanoparticles. This is due to the strong amphiphilic nature of CTAB, which enables it to orient at the oil-water interface and reduce interfacial tension, whereas silica nanoparticles are primarily hydrophilic and show limited interfacial activity.

As shown in Table 6, three single diluents are listed: crude palm oil, dibutyl carbitol, and n-heptane. The interfacial tension of each of the diluents with water is different. N-heptane, reported by Chakraborty et

al. [34], shows the lowest interfacial tension among these three diluents. The reason why n-heptane can lower the interfacial tension with water is probably due to the presence of carriers (D2EHPA), kerosene, and surfactant (Span 80). These chemicals were used to prepare the liquid membrane phase, so the interfacial tension reported by the researchers was a mixture of these chemicals with the diluents. Hence, instead of using a single diluent, the diluents may be mixed with other chemicals to further lower the interfacial tension with water. Adding nanoparticles or mixing diluents with other additive chemicals can reduce interfacial tension, leading to more stable emulsions. A more homogeneous and smaller emulsion globule is produced when there is lower interfacial tension, which lowers the energy barrier that needs to be overcome [35]. Smaller globules are preferred for the ELM process because they have greater stability against coalescence, larger interfacial area for mass transfer, and lower internal diffusion resistance [36].

Table 6. Interfacial tension on various types of diluents

Diluents	σ (mN/m)	References
Palm Oil + Fe_2O_3 nanoparticles	2	[7]
Toluene + Silica nanoparticles	32	[14]
Toluene + CTAB	12	[16]
Crude Palm Oil	8	[37]
Dibutyl Carbitol	12.24	[38]
n-heptane	2.35	[34]

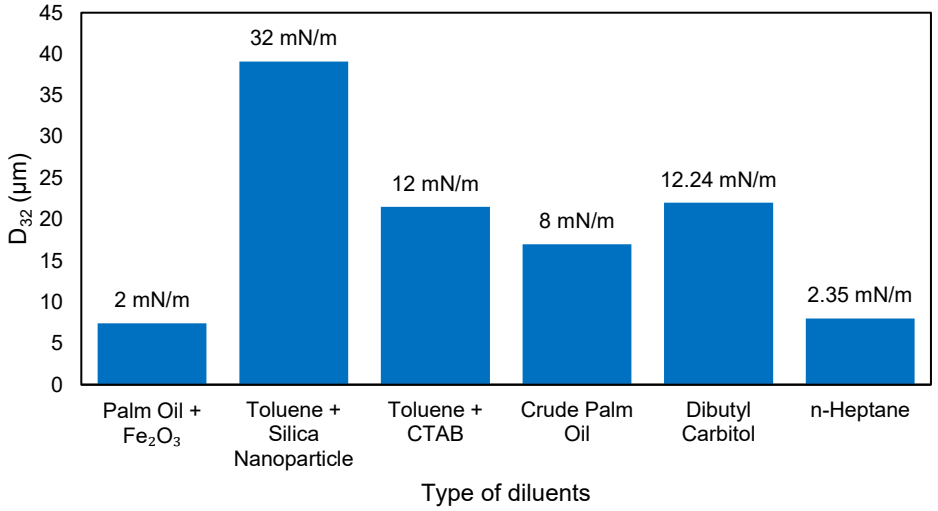

Figure 10. Effect of various diluents with different interfacial tension on globule size, D_{32}. (Fixed conditions: impeller diameter: 0.03 m; agitation speed: 5.00 s^{-1}; holdup fraction: 0.25; temperature: 26±1 ºC)

Effect of Holdup Fraction in Hinze-Kolmogorov Theory

The study investigated the impact of holdup fraction on emulsion globule size in the ELM process in the range of 0.01 – 0.35 which were obtained from Equation 7. The predicted globule size aligns closely with experimental data, where the percentage AARD between the experimental and predicted values is just 0.46%, showing the high accuracy of the empirical equation used to predict globule size. Holdup fraction represents the dispersion of primary emulsion (water-in-oil) to external feed phase by varying the external feed phase volume while fixing the primary emulsion volume. As the volume of external feed phase increases, the holdup fraction reduces, due to the wider distribution of emulsion globules. It was found that a higher holdup fraction leads to smaller globules, as shown in Table 7 and Fig. 11. This agrees with the experimental observations, where the emulsion size increased with increasing treat ratio, and the trend is quantitatively described by the empirical correlation (Equation 7). The effectiveness of extraction decreases as the external feed phase volume rises because the emulsion globules' distribution widens and their distance from one another increases, further reducing the interfacial area available per unit volume of the feed phase [30]. According to Abbassian and Kargari [39], when the holdup fraction increased from 0.0625 to 0.167, both the extraction rate and extraction efficiency increased by approximately 18%. This is because the mass transfer area is further enhanced as the number of

emulsion globules per unit volume of the mixture increases with the rise in emulsion volume. It may also result from a higher availability of stripping reagent for each solute molecule to react with, or from an increase in the ratio of stripping agent moles to solute molecules in the feed phase.

Table 7. The simulation and experimental results of varying external feed phase volume, V_f on Sauter mean diameter, D_{32}

Treatment ratio	Hold up fraction	Simulation	Experimental
1:1	0.500	Globules do not form	6.98
1:7	0.125	23.64	7.70
1:10	0.091	28.07	27.90
1:13	0.071	30.60	26.55
1:16	0.059	32.24	28.90
1:19	0.050	33.38	30.90

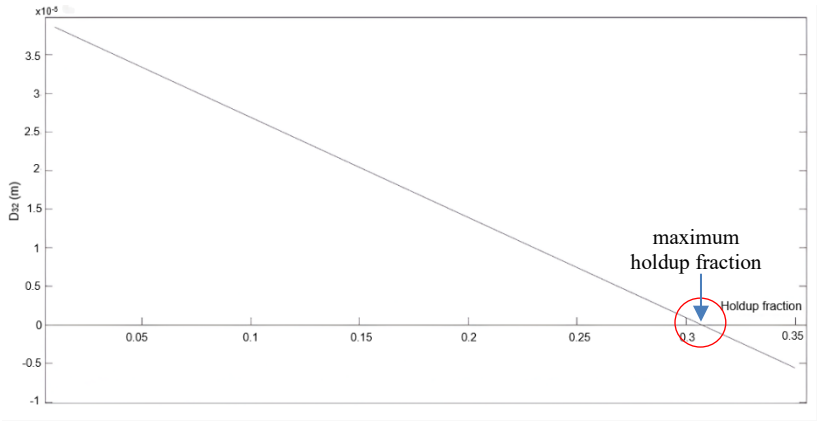

Figure 11. Effect of holdup fraction on globule size, D_{32}

The rise in emulsion holdup, which further expands the interfacial area for mass transfer, could be the other possible reason for emulsion stability [30]. In addition, smaller globules also have a lower coalescence tendency, which retains their stability and size [36]. However, there is a limit to how small the globules can be, as a too-high holdup fraction may cause excessive breakage and consequent coalescence, resulting in larger globules. The model is validated up to a maximum holdup fraction of 0.307. Table 7 and Fig. 12 show the simulation and experimental results at various holdup fractions with average AARD of 10.1%. Beyond the maximum holdup fraction, the globules did not form. This is due to the fact that an excessive amount of W/O emulsion causes poor emulsion dispersion in the feed phase. Similar trend was reported by Goyal et al. [40]. The researchers discovered that the optimum value for the treatment ratio during the chromium (Cr (VI)) removal process is 2 (v/v). The volume ratio of 3.33 (v/v) between the continuous phase and W/O emulsion was used by Djenouhat et al. [41] to ensure adequate spreading of primary emulsion during the external feed phase. Nevertheless, beyond the optimum value of holdup fraction, the formation of emulsion globules was decreased, caused by the osmotic pressure difference. Large amounts of W/O emulsion caused the migration of water molecule from external feed phase into the internal phase which led to swelling-breakage phenomenon. Moreover, it was noted that when the treatment ratio was set at one to one percent by volume (v/v), it was discovered that the limited interfacial area for mass transfer decreased the ELM performance. This could be because the big volume of the emulsion increased the overall viscosity of the W/O/W emulsion system, leading to an inversion in the interfacial area. Hence, the minimum possible emulsion volume is always favoured in order to get good ELM performance and better distribution of fine internal phase droplets in the external feed phase [42].

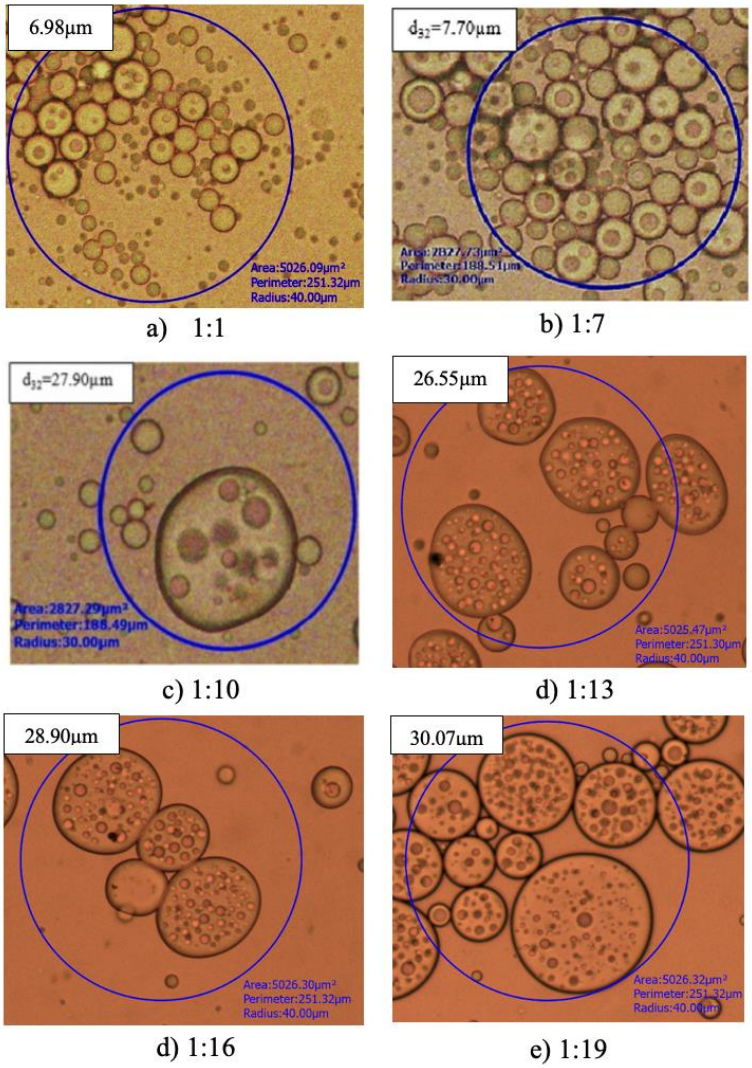

Figure 12. The illustration of the W/O/W emulsion formation for the effect of holdup fraction

Future Prospect of ELM Model

ELM Stability

ELM processes are a relatively advanced technique that has been thoroughly investigated for possible use in a variety of industries, including metal recovery and pollutant removal, but are hindered by instability under fluid shear leading to coalescence, swelling, and breakage. In the ELM W/O/W model, coalescence occurs when the internal phase within the liquid membrane phase merges into bigger ones through stages such as initial contact that facilitates attractive interactions, draining of the continuous phase film between droplets, breaking of this film, and final droplet merging. Predicting droplet coalescence is challenging because it depends on the molecular characteristics of droplet surfaces. To predict more accurate ELM globules sizes, the relation of primary emulsion model should be considered in future model development.

In addition, the swelling in ELM process happens when external feed phase diffuses into the oil droplets, which causes the emulsion volume to increase [43]. It includes osmotic swelling, caused by osmotic pressure differences, and entrainment swelling, resulting from the repeated coalescence and re-dispersion [44]. On the other hand, shear forces in the ELM process can cause emulsion breakage and may result in leakage of the internal phase into the external feed. Factors affecting ELM stability include surfactant type, carrier, temperature, pH value, globule size, residence time, ionic strength, solvent viscosity, and agitation speed [17, 45, 46]. Therefore, all these factors need to be considered in the model.

Impeller Type and Size

The size and formation of emulsion globules are significantly influenced by the type and configuration of the impeller. Impellers break down droplets into smaller globules by the generation of shear forces, thereby dispersing fluids and produce emulsions. The impeller's design and characteristics, such as its number of blades, size, and angle of blades, affect the shear rate, mixing intensity, and the size of the globules of emulsion. This is due to the increase of the capability to disperse the globules by the impeller per unit mass, and it is well-defined by the relationship between the impeller size and the mean globule diameter, $D_{32} \propto D_I^{-0.84}$. Therefore, the impeller type and size should be considered in the ELM W/O/W model.

Scaling Up of ELM Process

There is potential in enlarging the ELM process to an industrial level for wastewater treatment. Normally, engineers conduct pilot-scale studies to optimise process parameters like volume of surfactant, agitation speed and time, etc. then scaling up gradually to identify and mitigate the potential issues. For example, Kitagawa et al. [47] have proved through the results of laboratory and pilot plant that ELM technology is capable of reducing the levels of heavy metals ions like copper ions. The ELM W/O/W model could be used as a preliminary study to scale up the process. Therefore, the developed ELM model would play a crucial role to forecast the mean globule emulsion size when the process is scaled up into a wastewater treatment plant.

In order to extract the various solutes effectively, the ELM model plays an important role in predicting the extraction efficiency. It is an essential part in acquiring deep understanding about the chemical reaction and reactivity of the solutes. Hence, by considering all the parameters, the ELM W/O/W model can overcome stability challenges and enhance the scalability and stability of ELM process in industrial wastewater treatment and other applications.

Conclusion

The study successfully achieved its main goal of using the Hinze-Kolmogorov theory to predict globule size in ELM with assisted blended surfactant nanoparticles using MATLAB software. A new empirical equation was developed and validated, showing low AARD values of 3.41% and 1.04% for Case 1 and Case 2, respectively. Therefore, the empirical equation based on Hinze-Kolmogorov theory was created, and the values of C_1 and C_2 were obtained, which are 0.0436 and -3.2561, respectively. The study found that parameters like impeller diameter and agitation speed are inversely proportional to globule size, and that low interfacial tension and high holdup fractions lead to smaller globules. However, in the current work, there is an optimal holdup fraction beyond which no globules formed, and all the simulations based on theories may not be accurate beyond the optimal point; in practice, globule breakage and coalescence phenomena may occur. The model provides a practical tool for ELM design and optimization by enabling the selection of operating conditions that improve emulsion stability and reduce experimental trial-and-error. This predictive framework can guide ELM design, optimize operating conditions, and support future applications in scale-up, other metal extraction systems, and formulations with different surfactant-nanoparticle blends.

Conflicts of Interest

The authors declare that there is no conflict of interest regarding the publication of this paper.

Acknowledgment

This research was funded by Ministry of Higher Education Malaysia under Fundamental Research Grant Scheme (FRGS) (FRGS/1/2022/STG05/UTM/01/2). The authors would also like to acknowledge the Centre of Lipids Engineering and Applied Research (CLEAR) and Universiti Teknologi Malaysia for facility support to make this research possible.

References

[1] Rahman, D. Z., Vijayaraghavan, J., & Thivya, J. (2023). A comprehensive review on Zinc(II) sequestration from wastewater using various natural/modified low-cost agro-waste sorbents. *Biomass Conversion and Biorefinery,*

13(7), 5469–5499.
[2] Yang, K. J., Fong, L. L., Kee, C. M., & Saeed, A. A. (2022). Kinetic study for adsorption of heavy metals on zeolite. *Journal of Harbin Institute of Technology (New Series), 29*(1), 70–76.
[3] Hussaini, S., & Tita, A. M. (2023). Zinc and lead solvent extraction and electrowinning. In *The Minerals, Metals and Materials Series* (pp. 403–459). Springer. https://doi.org/10.1007/978-3-031-33934-4_15.
[4] Dąbrowski, A., Hubicki, Z., Podkościelny, P., & Robens, E. (2004). Selective removal of the heavy metal ions from waters and industrial wastewaters by ion-exchange method. *Chemosphere, 56*(2), 91–106. https://doi.org/10.1016/j.chemosphere.2004.03.006.
[5] Gulnaziya, I., Nicholas, Y. J., Mohammad, A. A., Farihahusnah, H., & Mohamed, K. A. (2020). Removal of zinc from wastewater through the reduction potential determination and electrodeposition using adsorption-desorption solutions. *Iranian Journal of Chemistry and Chemical Engineering, 39*(6), 121–130.
[6] Tan, S., Zhang, T., Cheng, C., Wang, Z., Li, H., & Zhao, Y. (2025). Efficient removal and stepwise recovery of various heavy metals from water by using calcium carbonate with different activity. *Separation and Purification Technology, 354,* 129142. https://doi.org/10.1016/j.seppur.2025.129142.
[7] Suliman, S. S., Othman, N., Noah, N. F. M., & Kahar, I. N. S. (2023). Extraction and enrichment of zinc from chloride media using emulsion liquid membrane: Emulsion stability and demulsification via heating-ultrasonic method. *Journal of Molecular Liquids, 374,* 121261. https://doi.org/10.1016/j.molliq.2023.121261.
[8] Kahar, I. N. S., Othman, N., Idrus-Saidi, S. A., Noah, N. F. M., Nozaizeli, N. D., & Suliman, S. S. (2024). Integrated emulsion liquid membrane process for enhanced silver recovery from copper-silver leached solution. *Chemical Engineering Research and Design, 212,* 434–444. https://doi.org/10.1016/j.cherd.2024.02.004.
[9] Suliman, S. S., Othman, N., Noah, N. F. M., Johari, K., & Ali, N. A. (2022). Stability of primary emulsion assisted with nanoparticle in emulsion liquid membrane process for zinc extraction. *Materials Today: Proceedings, 65,* 3081–3092. https://doi.org/10.1016/j.matpr.2022.03.559.
[10] Yan, J., & Pal, R. (2001). Osmotic swelling behavior of globules of W/O/W emulsion liquid membranes. *Journal of Membrane Science, 190*(1), 79–91. https://doi.org/10.1016/S0376-7388(01)00404-6.
[11] Mohammed, A. A., Atiya, M. A., & Hussein, M. A. (2020). Removal of antibiotic tetracycline using nano-fluid emulsion liquid membrane: Breakage, extraction and stripping studies. *Colloids and Surfaces A: Physicochemical and Engineering Aspects, 595,* 124680. https://doi.org/10.1016/j.colsurfa.2020.124680.
[12] Sun, Z., Yan, X., Xiao, Y., Hu, L., Eggersdorfer, M., Chen, D., Yang, Z., & Weitz, D. A. (2022). Pickering emulsions stabilized by colloidal surfactants: Role of solid particles. *Particuology, 64,* 153–163. https://doi.org/10.1016/j.partic.2022.03.003.
[13] Esmaeilzadeh, P., Hosseinpour, N., Bahramian, A., Fakhroueian, Z., & Arya, S. (2014). Effect of ZrO_2 nanoparticles on the interfacial behavior of surfactant solutions at air–water and n-heptane–water interfaces. *Fluid Phase Equilibria, 361,* 289–295. https://doi.org/10.1016/j.fluid.2013.11.020.
[14] Raji-Asadabadi, M., Abolghasemi, H., Maragheh, M. G., & Davoodi-Nasab, P. (2013). On the mean drop size of toluene/water dispersion in the presence of silica nanoparticles. *Chemical Engineering Research and Design, 91*(9), 1739–1747. https://doi.org/10.1016/j.cherd.2013.02.016.
[15] Fujii, S., Okada, M., & Furuzono, T. (2007). Hydroxyapatite nanoparticles as stimulus-responsive particulate emulsifiers and building block for porous materials. *Journal of Colloid and Interface Science, 315*(1), 287–296. https://doi.org/10.1016/j.jcis.2007.07.047.
[16] Davoodi-Nasab, P., Abolghasemi, H., Safdari, J., & Raji-Asadabadi, M. (2014). Mean drop size in the presence of cetyl trimethyl ammonium bromide in horizontal mixer settler. *Asia-Pacific Journal of Chemical Engineering, 9*(1), 93–104. https://doi.org/10.1002/apj.1785.
[17] Othman, N., Kahar, I. N. S., Long, S. S., Noah, N. F. M., Idrus-Saidi, S. A., & Suliman, S. S. (2024). Prediction of zinc extraction from aqueous solution using iron oxide nanoparticles embedded formulation for tuning emulsion liquid membrane stability. *Chemical Engineering Research and Design, 204,* 572–584. https://doi.org/10.1016/j.cherd.2024.01.015.
[18] Suliman, S. S., Othman, N., Noah, N. F. M., Jusoh, N., & Sulaiman, R. N. R. (2021). Empirical correlation of emulsion size prediction for zinc extraction using flat blade impeller system in emulsion liquid membrane process. *Malaysian Journal of Fundamental and Applied Sciences, 17*(6), 742–751.
[19] Jusoh, N., Othman, N., Ambi, L. L. A. A., Noah, N. F. M., Rosly, M. B., & Rahman, H. A. (2022). Empirical correlation of stable double emulsion system of organic compound extraction in emulsion liquid membrane process. *Malaysian Journal of Fundamental and Applied Sciences, 18,* 197–205.
[20] Zhao, P., Fan, W., Zhang, L., & Nan, G. (2013). Study on influencing factors on particle size and stability of asphalt emulsion and their correlation. *Petroleum Processing and Petrochemicals, 44*(7), 12–16.
[21] Farsoiya, P. K., Liu, Z., Daiss, A., Fox, R. O., & Deike, L. (2023). Role of viscosity in turbulent drop break-up. *Journal of Fluid Mechanics, 972,* A11-1–A11-17. https://doi.org/10.1017/jfm.2023.345.
[22] Khakpay, A., Abolghasemi, H., & Salimi-Khorshidi, A. (2009). The effects of a surfactant on mean drop size in a mixer-settler extractor. *Chemical Engineering and Processing: Process Intensification, 48*(6), 1105–1111. https://doi.org/10.1016/j.cep.2009.03.010.
[23] Lee, J. M., & Soong, Y. (1985). Effects of surfactants on the liquid–liquid dispersions in agitated vessels. *Industrial & Engineering Chemistry Process Design and Development, 24*(1), 118–121. https://doi.org/10.1021/i200023a022.
[24] El-Hamouz, A., Cooke, M., Kowalski, A., & Sharratt, P. (2009). Dispersion of silicone oil in water surfactant solution: Effect of impeller speed, oil viscosity and addition point on drop size distribution. *Chemical Engineering and Processing: Process Intensification, 48*(2), 633–642. https://doi.org/10.1016/j.cep.2008.09.002.
[25] Desnoyer, C., Masbernat, O., & Gourdon, C. (2003). Experimental study of drop size distributions at high phase ratio in liquid–liquid dispersions. *Chemical Engineering Science, 58*(7), 1353–1363. https://doi.org/10.1016/S0009-2509(03)00016-6.
[26] Khakpay, A., Abolghasemi, H., & Montazer-Rahmati, M. M. (2010). The effect of sodium dodecyl sulfate on mean drop size in a horizontal mixer–settler extractor. *The Canadian Journal of Chemical Engineering, 88*(1), 101–108. https://doi.org/10.1002/cjce.20349.

[27] Noah, N. F. M., Othman, N., & Binanga, H. (2022). Prediction of zinc extraction using facilitated emulsion liquid membrane model. *Malaysian Journal of Fundamental and Applied Sciences, 18*(2), 206–217.
[28] Pandey, S. (2023). Optimization of PID controller parameters for speed control of DC motor using firefly and fminsearch algorithms. *SSRN*. https://doi.org/10.2139/ssrn.4378784.
[29] Ohtake, T., Hano, T., Takagi, K., & Nakashio, F. (1987). Effects of viscosity on drop diameter of W/O emulsion dispersed in a stirred tank. *Journal of Chemical Engineering of Japan, 20*(5), 443–447. https://doi.org/10.1252/jcej.20.443.
[30] Kumar, A., Thakur, A., & Panesar, P. S. (2019). A review on emulsion liquid membrane (ELM) for the treatment of various industrial effluent streams. *Reviews in Environmental Science and Bio/Technology, 18*(1), 153–182. https://doi.org/10.1007/s11157-018-9505-3.
[31] Hussein, M. A., Mohammed, A. A., & Atiya, M. A. (2019). Application of emulsion and Pickering emulsion liquid membrane technique for wastewater treatment: An overview. *Environmental Science and Pollution Research, 26*(36), 36184–36204. https://doi.org/10.1007/s11356-019-06622-8.
[32] Cheraghian, G., & Hendraningrat, L. (2016). A review on applications of nanotechnology in the enhanced oil recovery part A: Effects of nanoparticles on interfacial tension. *International Nano Letters, 6,* 129–138. https://doi.org/10.1007/s40089-016-0178-0.
[33] Vignati, E., Piazza, R., & Lockhart, T. P. (2003). Pickering emulsions: Interfacial tension, colloidal layer morphology, and trapped-particle motion. *Langmuir, 19*(17), 6650–6656. https://doi.org/10.1021/la034170t.
[34] Chakraborty, M., Bhattacharya, C., & Datta, S. (2003). Effect of drop size distribution on mass transfer analysis of the extraction of nickel(II) by emulsion liquid membrane. *Colloids and Surfaces A: Physicochemical and Engineering Aspects, 224*(1), 65–74. https://doi.org/10.1016/S0927-7757(03)00344-3.
[35] Schroën, K., de Ruiter, J., & Berton-Carabin, C. (2020). The importance of interfacial tension in emulsification: Connecting scaling relations used in large scale preparation with microfluidic measurement methods. *ChemEngineering, 4*(4), 63. https://doi.org/10.3390/chemengineering4040063.
[36] Peng, L., Yang, M., Guo, S. S., Liu, W., & Zhao, X. Z. (2011). The effect of interfacial tension on droplet formation in flow-focusing microfluidic device. *Biomedical Microdevices, 13*(3), 559–564. https://doi.org/10.1007/s10544-011-9543-0.
[37] Chow, M. C., & Ho, C. C. (2000). Surface active properties of palm oil with respect to the processing of palm oil. *Journal of Oil Palm Research, 12*(1), 107–116.
[38] Javanshir, S., Abdollahy, M., & Abolghasemi, H. (2012). Drop size distribution in a mixer–settler reactor for the gold chloride/DBC system. *Chemical Engineering Research and Design, 90*(10), 1680–1686. https://doi.org/10.1016/j.cherd.2012.01.016.
[39] Abbassian, K., & Kargari, A. (2016). Effect of polymer addition to membrane phase to improve the stability of emulsion liquid membrane for phenol pertraction. *Desalination and Water Treatment, 57*(7), 2942–2951. https://doi.org/10.1080/19443994.2015.1070542.
[40] Goyal, R. K., Jayakumar, N. S., & Hashim, M. A. (2011). A comparative study of experimental optimization and response surface optimization of Cr removal by emulsion ionic liquid membrane. *Journal of Hazardous Materials, 195,* 383–390. https://doi.org/10.1016/j.jhazmat.2011.08.036.
[41] Djenouhat, M., Hamdaoui, O., Chiha, M., & Samar, M. H. (2008). Ultrasonication-assisted preparation of water-in-oil emulsions and application to the removal of cationic dyes from water by emulsion liquid membrane: Part 2. Permeation and stripping. *Separation and Purification Technology, 63*(1), 231–238. https://doi.org/10.1016/j.seppur.2008.02.014.
[42] Kulkarni, P. S., & Mahajani, V. V. (2002). Application of liquid emulsion membrane (LEM) process for enrichment of molybdenum from aqueous solutions. *Journal of Membrane Science, 201*(1), 123–135. https://doi.org/10.1016/S0376-7388(01)00624-5.
[43] Jusoh, N., Othman, N., Sulaiman, R. N. R., Noah, N. F. M., & Zaini, M. A. A. (2022). Optimization of synergistic green emulsion liquid membrane stability for enhancement of silver recovery from aqueous solution. *Korean Journal of Chemical Engineering, 39*(2), 423–430. https://doi.org/10.1007/s11814-021-0932-5.
[44] Wan, Y., & Zhang, X. (2002). Swelling determination of W/O/W emulsion liquid membranes. *Journal of Membrane Science, 196*(2), 185–201. https://doi.org/10.1016/S0376-7388(01)00723-1.
[45] Jusoh, N., & Othman, N. (2016). Stability of water-in-oil emulsion in liquid membrane prospect. *Malaysian Journal of Fundamental and Applied Sciences, 12*(3), 114–116.
[46] Kahar, I. N. S., Ali, A. S., Othman, N., Noah, N. F. M., & Suliman, S. S. (2023). Copper extraction using LIX 84 as a mobile carrier in the emulsion liquid membrane process. *Journal of Applied Membrane Science & Technology, 27*(3), 69–80. https://doi.org/10.3968/j.amst.2023.27.3.69.
[47] Kitagawa, T., Nishikawa, Y., Frankenfeld, J., & Li, N. (1977). Wastewater treatment by liquid membrane process. *Environmental Science & Technology, 11*(6), 602–605. https://doi.org/10.1021/es60132a011.